energies

MDPI

Article

Consistency Testing Method for Energy Storage Systems with Time-Series Properties

Nan Wang and Zhen Li *

State Grid Integrated Energy Services Group Limited, Xicheng District, Beijing 100032, China; sgcc_nanwang@163.com
* Correspondence: sgcc_zhenli@163.com

Abstract

As a cushion for the volatility of renewable energy, energy storage systems can achieve peak shaving and valley filling, thereby improving the operational efficiency and economic performance of the power grid. In addition, energy storage systems can absorb renewable energy production, thereby enhancing the safety and reliability of the electrical power system. Nowadays, energy storage systems are facing severe problems such as explosions that are caused by overcharging and discharging. The main reason for the overcharging and discharging of energy storage systems is the inconsistency in the state of the electric core in the charging and discharging process, which not only affects the safety of the electric core, but also influences the overall charging and discharging capacity of the energy storage system. To address this inconsistency of energy storage cores, this paper proposes an energy storage consistency monitoring method under the framework of clustering-classification, which adopts the Belief Peaks Evidential Clustering and Evidential K-Nearest Neighbors classification algorithm. This paper proposes a BPEC-EKNN-based method for battery inconsistency detection and localization. The proposed approach first constructs battery performance evaluation coefficients to characterize inter-cell behavioral differences, and then integrates an enhanced k-nearest neighbor strategy to identify abnormal cells. It also identifies and locates inconsistent battery cells by analyzing the magnitude of the confidence level m (Ω), without relying on predefined thresholds. Also, time-series data as opposed to the evaluation of voltage data at a singular point is engaged to realize the detection and localization of energy storage core consistency anomalies under the consideration of time-series data. The proposed algorithm is capable of identifying inconsistencies among energy storage batteries, with the parameter m (Ω) serving as an indicator of the likelihood of inconsistency. Experimental results on battery pack datasets demonstrate that the proposed method achieves higher detection accuracy and robustness compared with representative statistical threshold-based methods and machine learning approaches, and it can more accurately identify inconsistent battery cells. By applying perturbation analysis to real-time operational data, the algorithm proposed in this paper can detect inconsistencies in battery cells reliably.

Keywords: energy storage systems; consistency detection; clustering; classification algorithms

Check for updates

Academic Editor: King Jet Tseng

Received: 3 November 2025
Revised: 16 December 2025
Accepted: 18 December 2025
Published: 21 December 2025

Copyright: © 2025 by the authors. Licensee MDPI, Basel, Switzerland. This article is an open access article distributed under the terms and conditions of the Creative Commons Attribution (CC BY) license.

1. Introduction

Against the backdrop of the global energy transition toward clean and low-carbon sources [1], renewable energy has emerged as a future direction of energy development due to its environmental friendliness and resource renewability [2]. However, the inherent

volatility and randomness of renewable energy sources like solar and wind power result in intermittent electricity generation. This unpredictable energy flow poses challenges for stable and continuous grid integration, potentially compromising grid security. Energy storage systems play a crucial role in flexibly regulating power distribution, thereby ensuring the stable operation of the power grid [3].

Energy storage is a device capable of bidirectional conversion between electrical and chemical energy, playing an indispensable regulatory role in energy systems. It effectively smooths fluctuations in renewable energy output and balances peak-to-valley variations in user loads, significantly reducing curtailment of wind and solar power while enhancing the reliability and stability of energy system operations [4–6]. As energy storage technologies become increasingly applied in the energy sector, safety concerns have also grown more prominent. Safety incidents triggered by abnormal operating conditions such as overcharging and over-discharging occur frequently, not only causing economic losses but also posing serious threats to public safety. According to the incomplete statistics of the industry database of China Chemical and Physical Power Supply Association (CESA), 87 accidents have occurred in energy storage power stations since November 2009, including user-side, power-side, grid-side, and other types of energy storage power stations. On 5 September 2024, one of the 24 battery storage containers of the U.S. San Diego Gas & Electric Company (SDG&E) caught fire; on 10 September 2024, a lithium battery exploded in Ali Yun's Niigata Phi data center, causing service disruptions for related technology companies; and on 23 September 2024, a lithium battery container caught fire at the Port of Montreal terminal in Canada. In recent years, as the share of energy storage in the energy system has increased, the number of accidents related to energy storage systems has also increased.

The safety of energy storage systems diminishes with increasing charge–discharge cycles and aging of insulating components [7–9]. Therefore, real-time status monitoring and fault detection are critical for energy storage systems. From the perspective of energy storage system structure, the battery system is the core of the entire energy storage system [10], which is composed of hundreds of electric cells connected in series and parallel. To meet load voltage and power requirements, hundreds or thousands of cells connected in series and parallel form the core of the energy storage system—the battery pack. Due to minute variations in cell manufacturing and the impact of different operating environments, inconsistencies arise in internal cell impedance and charge and discharge states. To prevent overcharging and over-discharging, the performance and lifespan of energy storage systems are constrained by the weakest cell [11], adhering to the law of the least. This significantly impacts the charging and discharging efficiency of the energy storage system [12].

Therefore, analyzing and researching the consistency of energy storage systems holds significant practical and applied value [13,14]. From the current state of research, studies on the consistency of energy storage systems remain relatively scarce, with most focusing on fault identification and early warning for these systems.

For consistency monitoring [15], the methodology can be divided into statistical-based methods and machine learning-based methods [11]. Although these techniques have been widely studied, their limitations motivate the development of more robust and uncertainty-aware solutions.

Statistical methods, such as differential voltage analysis, standard deviation monitoring, and rule-based thresholds, are computationally efficient and easy to implement. However, their performance heavily depends on manually defined thresholds, which are sensitive to operating conditions, noise levels, and aging states. As a result, these methods often suffer from either excessive false alarms or missed detections when ap-

plied to large-scale energy storage systems with dynamic load profiles. More importantly, threshold-based techniques typically provide binary decisions without quantifying uncertainty, limiting their reliability in early-stage or borderline inconsistency scenarios.

Machine learning-based approaches attempt to overcome rigid thresholds by learning data patterns automatically. Clustering and distance-based methods can capture similarity relationships among cells, while supervised models achieve high accuracy under labeled conditions. Nevertheless, most existing ML methods implicitly assume clean data and balanced samples, and their decisions are often opaque and deterministic. In practice, battery data are noisy, incomplete, and affected by operational variability, which can significantly degrade model stability. Moreover, many ML approaches focus on classification accuracy alone and lack mechanisms to explicitly represent uncertainty, making them vulnerable to misclassification when cell behaviors overlap.

The most used statistical-based method is the threshold method, which establishes safety threshold ranges for critical parameters such as voltage and temperature, continuously monitoring deviations between individual cells and the average performance of the energy storage system. This approach relies heavily on the rationality of threshold selection and parameter choice, requiring adjustments to thresholds over time and based on charge and discharge states. The machine learning-based methods can be summarized into several steps, including data acquisition, feature calculation and extraction, and inconsistent evaluation [11]. In the data acquisition process, signals such as voltage and temperature are acquired. During the feature calculation and extraction stage, parameters such as state of charge and internal resistance are calculated, and parameters irrelevant to consistency diagnosis are removed. In the inconsistent evaluation phase, two types of evaluation methods, regression methods and classification methods, are used for evaluation. Ref. [16] proposes a data-driven method with charging rate, temperature, state of charge, and accumulated driving mileage as the inputs. Ref. [17] adopts a capacity model based on the charging process for state of health estimation of lithium ion batteries. Ref. [18] proposes an accurate charging model of battery energy storage, which closely approximates the real-life battery charging constraints, and this method is also a consistency detection method under laboratory conditions. Ref. [19] designs a cyclic aging experiment scheme, and parameters such as open-circuit voltage, ohmic resistance, polarization resistance, and capacitance can be obtained during the experimental process. The parameter distributions are analyzed and merged as a decision method for consistency diagnosis. Ref. [20] identifies ohmic internal resistance, electrochemical polarization internal resistance, and concentration difference polarization internal resistance from the real-time operating data. With the identified parameters, an improved autoregressive method is proposed to recognize inconsistencies. Ref. [21] proposes a novel predictive energy management paradigm guided by deep reinforcement learning. By optimizing action space selection based on the degradation characteristics of the fuel cell (FC) system, the lifespan of FC is extended by 16.50%. Ref. [22] proposes a novel energy management paradigm to achieve the comprehensive control of cabin comfort and fuel cell/battery durability. A twin delayed deep deterministic policy gradient algorithm is proposed in this paper, and the battery life is extended by at least 3.79%.

In summary, the current real-time inconsistency diagnostic methods for energy storage systems have low reliability, high misclassification rate, or no offline diagnostic methods, and there is no practical and highly accurate method for monitoring the consistency of energy storage system cores. Also, the majority of algorithms initially calculate parameters such as state of charge and internal resistance. By analyzing the distribution of these calculated parameters, the inconsistencies of cells can be identified. Nevertheless, the estimation of such parameters is typically subject to a certain degree of error, and such

errors can also affect the consistency diagnosis results. Taking this into consideration, this paper proposes a consistency diagnosis method based on measurable parameters, in which the measurable parameters refer to voltage mostly. This paper proposes a consistency monitoring method for energy storage systems within a clustering-classification framework. The method employs peak confidence clustering to extract features from sample data and utilizes classification algorithms to characterize the probability of a cell belonging to a specific category or remaining unclassified. The validation results demonstrate that the algorithm can detect inconsistencies of cells accurately, and provide the confidence level m (Ω) to measure the probability of inconsistencies.

2. Belief Peaks Evidential Clustering

The clustering algorithm used in this paper is Belief Peaks Evidential Clustering (BPEC), which is an improved algorithm based on density peak clustering (DPC). The density peak clustering algorithm is a method proposed by Alex Rodriguez in 2014 [23,24], and its basic idea is that the density of points around the class centers is high and the distance between the class centers is relatively high. The number of points within a region is regarded as density.

$$\rho_i = \sum_{i \neq j} \chi(d_{ij} - d_c) \tag{1}$$

$$\chi(x) = \begin{cases} 1 & x < 0 \\ 0 & x \geq 0 \end{cases} \tag{2}$$

where ρ_i is the density of point i, d_{ij} is the distance between point i and point j, and d_c is the cutoff distance. Here, $x = d_{ij} - d_c$ is the argument of the indicator function $\chi(\cdot)$.

The relative distance is calculated as the minimum distance between the point and a point with a greater density than that of the point:

$$\delta_i = \min_{j:\rho_j > \rho_i} (d_{ij}) \tag{3}$$

where, for the sampling point with the highest density in the data, since no point with higher density can be found, its relative distance is the maximum distance between this point and all other points:

$$\delta_i = \max_{i \neq j} (d_{ij}) \tag{4}$$

A decision map is displayed by calculating the density and distance of all sample points; the upper right corner of the decision map, which has high density and distance, is regarded as the center of the clustering. By following the above process, the algorithm can automatically determine the number of categories in the clustering process.

The BPEC algorithm is a clustering algorithm proposed on the basis of DPC [25], by changing the density of the DPC algorithm to the confidence of becoming a class center based on the surrounding K nearest neighbors and their distances, which is discounted by evidence fusion.

The theory of evidence, Dempster–Shafer theory [26,27], was first proposed by Dempster in 1967 and then further refined by Shafer. The main difference between this theory and other algorithms is its ability to characterize imprecision and uncertainty. The theory differs from probabilistic theories in that it characterizes ignorance using a recognition framework Ω, which is the set of all possible values. Based on laws such as Dempster's

fusion, evidence fusion is used to process the effective new emergences that can be provided by different nearest neighbors into decisionable *BetP* probability measures:

$$BetP_m(\{\omega_q\}) = \sum_{\{A \subseteq \Omega \mid \omega_q \in A\}} \frac{m(A)}{|A|} = m(\{\omega_q\}) + \frac{m(\Omega)}{c} \tag{5}$$

where A is the value of the sample point, and in the clustering algorithm is whether a point is a sample point or not.

The main steps of the BPEC algorithm include determining the clustering centers and confidence divisions. The clustering center is determined by calculating the relative distance and confidence for each sample point, where the relative distance is consistent with the calculation of the DPC algorithm, and the confidence is calculated by searching for the K nearest neighbors with their closest distances around the sample point to be determined, calculating the Euclidean distances between the K nearest neighbors and the sample point to be determined, respectively, and discounting them into one piece of evidence:

$$\phi(d_i) = e^{-\gamma d_i^2} \tag{6}$$

where γ is the discount factor.

The K pieces of evidence available from the K nearest neighbors are fused to obtain the likelihood of the band determining the point to be the center of the class, the confidence level. The confidence and relative distance of each sample are used as the x-axis and y-axis to draw the decision diagram, respectively, and the sample point in the upper right corner of the decision diagram, the point with higher relative distance and confidence, is the class center. After completing the positioning of the class center, the confidence and recognition frame evidence of the sample points to be classified for each class can be calculated based on the relative distance of the sample points from the class center.

3. Evidential K-Nearest Neighbors Classification

On the basis of BPEC, the confidence of sample points for each category can be obtained, based on which the sample points to be judged are classified using the Evidential K-Nearest Neighbors (EKNN) algorithm. The EKNN classification algorithm was proposed by Denoeux [28], which is mainly used for the classification of data with imprecise and uncertain information, and its basic concept is input similarity and output similarity. The kernel of this algorithm is the KNN algorithm, which determines the category information according to the category attributes of the K nearest neighbors around the point to be classified, and it is a hard classification. The EKNN algorithm exploits the information of the nearest neighbor points, including the distance, category, and other information on the basis of this algorithm.

The algorithm faces the situation where some sample points cannot be classified during the classification process, and its confidence for each class is at a low level, while most of the confidence is assigned to the identification frame Ω.

The specific steps of the algorithm are as follows: for the point to be classified, its distance from all points in the sample space is calculated, and K nearest neighbors is selected in accordance with the distance from the closest to the farthest; according to the distance between the point and the K nearest neighbors, based on Formula (6), the distance is converted into evidence. The K pieces of evidence obtained from the K nearest neighbors are fused:

$$m^s = \bigoplus_{i \in I_k^s} m(A|x_i) \tag{7}$$

Taking the nearest neighbors of x_s as an example, their confidence that x_s belongs to the category q is

$$m^s(\{\omega_q\}) = K_1^{-1}\left\{\prod_{i\in I_k^s}\left[\alpha\phi(d_{s,i})m_i\left(\{\omega_q\}\right) + (1-\alpha\phi(d_{s,i}))\right] - \prod_{i\in I_k^s}(1-\alpha\phi(d_{s,i}))\right\} \quad (8)$$

where K_1 is the normalization factor, I is the nearest neighbor, $d_{s,i}$ is the Euclidean distance between x_s and x_i, and α is the algorithm hyperparameter.

The confidence that x_s belongs to the identification framework Ω that can be provided by the nearest neighbors of x_s is

$$m^s(\Omega) = K_1^{-1}\prod_{i\in I_k^s}(1-\alpha\phi(d_{s,i})) \quad (9)$$

4. BPEC-EKNN-Based Consistency Monitoring Method for Energy Storage Cores

The main steps of the method are as follows:

(1) Data collection, screening, and preliminary fault filtering. Collect and organize all parameters of the battery cells in the energy storage system, selecting key measurable parameters (primarily voltage) that characterize consistency status. The data is structured as time-series samples of fixed duration (e.g., 2 h windows) to capture charging/discharging dynamics.

During preprocessing, a preliminary fault filtering step is applied to remove cells exhibiting clear hardware or sensor failures, which could otherwise contaminate the dataset and inflate uncertainty in subsequent analysis. This filtering targets two types of evident faults: (i) voltages outside the physical operating range (3.0–3.7 V for the studied lithium-ion cells, based on manufacturer specifications), and (ii) extreme outliers deviating from the pack average by more than 3 standard deviations (σ), corresponding approximately to >0.1 V in this dataset, indicative of sensor malfunctions rather than operational inconsistencies.

This step is not intended for inconsistency detection but serves as a standard data quality assurance measure, akin to outlier removal in statistical analysis, ensuring the BPEC-EKNN algorithm focuses on subtle, operationally relevant inconsistencies rather than gross errors.

(2) Confidence and relative distance calculation. For each cell sample point (represented as a time-series voltage vector over a fixed window, e.g., 2 h), compute the relative distance δ using Equations (3) and (4) inherited from the DPC framework, and the confidence (belief) using the BPEC-specific evidence fusion in Equations (5) and (6). Plot the decision diagram with relative distance as the *x*-axis and confidence as the *y*-axis, and select points in the upper right corner as cluster centers, determining the number of cell state classes accordingly.

(3) Confidence classification and evidence base construction. According to the class centers obtained in step (2), calculate the relative distance of each cell sample point to each class center, and convert the distance to evidence according to Equation (6). Calculate the evidence of each sample point to each class and recognition framework, and use it as the battery evidence base TR.

(4) Neighborhood search for points to be classified. For each point to be classified, calculate its Euclidean distance from all points in the Battery Evidence Repository TR and use this as a basis to find its K nearest neighbors in the Battery Evidence Repository TR.

(5) Evidence fusion. Calculate the K nearest neighbors of the point to be classified (cell characteristic parameters) found in the battery evidence base TR in terms of distance, discount this distance according to Equation (6) to obtain K pieces of evidence, and fuse the K pieces of evidence according to Equations (7)–(9).

(6) Consistency monitoring. Based on the fused evidence, calculate the evidence that a cell belongs to each category and the identification framework evidence m (Ω); if m (Ω) is large, it indicates that the cell is an inconsistent cell; otherwise, it is a consistent cell.

The overall procedure of the proposed BPEC-EKNN method is summarized in Algorithm 1.

The pseudo-code for the BPEC-EKNN algorithm is as follows:

Algorithm 1. BPEC-EKNN

Input: K, α, γ, δ_{min}, bel_{min}, voltage of cells (2 h time span)

repeat
  Dividing training samples (90%) and test samples (10%)
  For training samples, calculate degrees of belied of all cells with (5) and (6)
  Calculate delta of all training cells with (4) and (5)
  Draw the decision graph, and determine δ_{min} and bel_{min} values based on the distribution of points
  Determine cluster centers v_c and credal partition
  For testing samples, determining the k nearest neighbors of a sample point
  Calculate m(Ω) of all testing cells with (7)–(9)
  Update the training and test sets
Until all battery cells have been classified

5. Simulation and Analysis

5.1. Energy Storage System and Data

In this paper, an energy storage power station, called the Guantang energy storage system in the Jinhu area of Jiangsu Province, is selected as an example to analyze and validate the proposed BPEC-EKNN algorithm. The critical hyperparameters K, γ, and α are selected as 20, 0.95, and 1.0. The Guantang Energy Storage Power Station consists of 16 battery compartments, with two units in each compartment. Each unit contains 7 battery clusters, and each cluster contains 238 individual cells. In this paper, a battery unit in the energy storage system is selected for analysis, which includes 7 battery clusters, and each cluster has 238 cells. Each cell has a voltage measurement point and every 4 cells have a temperature measurement point. Since the temperature measured by the temperature measurement point is greatly affected by environmental factors, cell arrangement, location of the measurement point, heat dissipation, and other factors, which cannot accurately characterize the inconsistency of the cells, this paper selects the voltage as the key characteristic parameter for consistency monitoring. A total of 238 cells in a day's voltage changes are shown in Figure 1.

Within this framework, 90% of the cells are allocated for clustering, while the remaining 10% are designated for classification. To ascertain the value of m (Ω) for each cell, it is necessary to execute 10 cycles. In each iteration of the process, 10% of the cells are selected randomly for classification, while the remaining 90% proceed to clustering. In the subsequent iteration, 10% of the cells from the unclassified pool are selected for classification, with the remaining 90% serving as the clustering sample. This process is repeated over 10 iterations, enabling the classification of all cells and the calculation of their values of m (Ω).

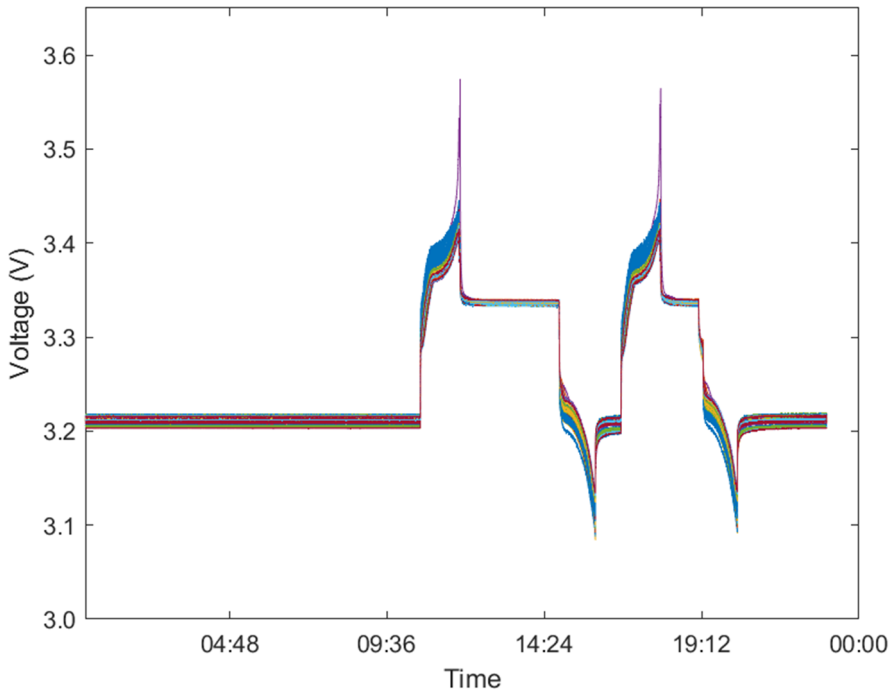


Figure 1. Voltage variation curve of each cell in the battery cluster.

5.2. BPEC-Based Clustering of Cell Parameters

The concept of battery consistency typically refers to the uniformity of characteristics within an entire cluster of batteries. Consequently, when assessing consistency, each cluster of 238 cells undergoes an overall cluster analysis. A two-hour time window is selected for each analysis to assess the consistency of each cell within that period. For this battery cluster of 238 cells, 10% of the cells are used as test data and 90% of the cells are used as training data. The BPEC algorithm is used to cluster the data of the cells used as training and the clustering decision diagram is shown in Figure 2. From the decision diagram, the two points on the upper right corner are the clustering centers. Since the numerical values between the two points differ only slightly, they are positioned in an overlapping state, with their respective [distance, belief] being [45.0817, 0.4333] and [45.0817, 0.4344], where the class center is shown in Figure 3. From the class center results, it can be seen that most of the batteries are at a more consistent level from the perspective of a day's time scale, and thus the distance between the two class centers does not differ much. The overall consistency is good. The clustering results also indicate that the differences between batteries are relatively minor during idle periods, whereas the variations among batteries are significant during charging and discharging processes.

The clustering results in Figure 3 also show that if the time span is selected to be too long, it will hide the inconsistency of the cell in some time periods, resulting in the inconsistency in charging or discharging time periods not being easily detected. In this way, it is necessary to cluster the data on the characteristics of the battery cells in a shorter time span. In this paper, 2 h is selected as the time span to analyze the changes in the characteristic parameters within the 2 h range. Taking 10–12 h as an example, the results of clustering using BPEC are shown in Figures 4 and 5. As can be seen from the figures, the overall relative distance is somewhat reduced due to the reduction in the amount of time-scale data from 24 h to 2 h for the time-series data. From the decision diagram (Figure 4), there are two class centers in the upper right corner. From the charging period clustering results (Figure 5), it can be seen that there are some gaps between the class centers, and they are mainly concentrated in the charging period.

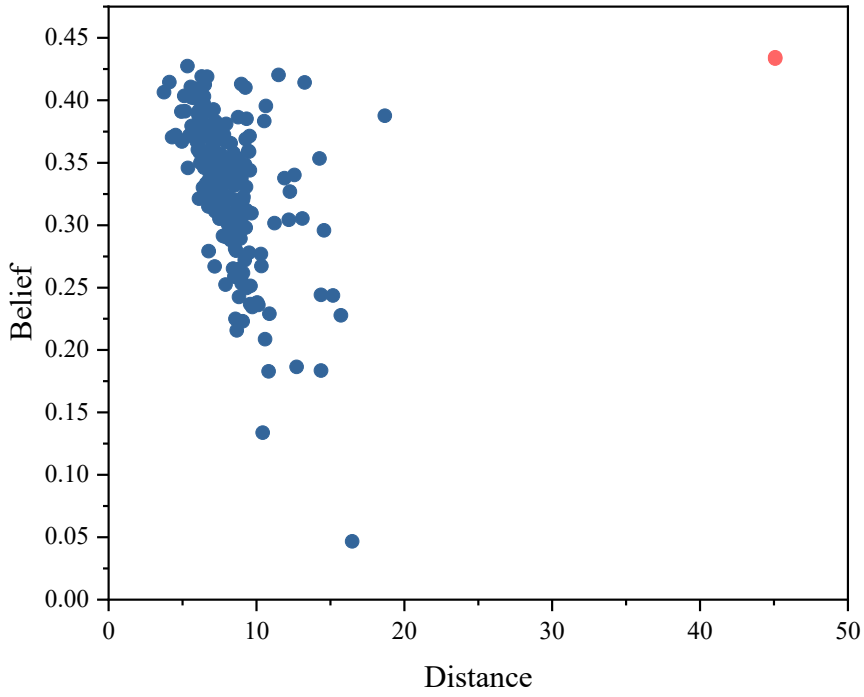


Figure 2. Clustering decision diagram of the battery cluster.

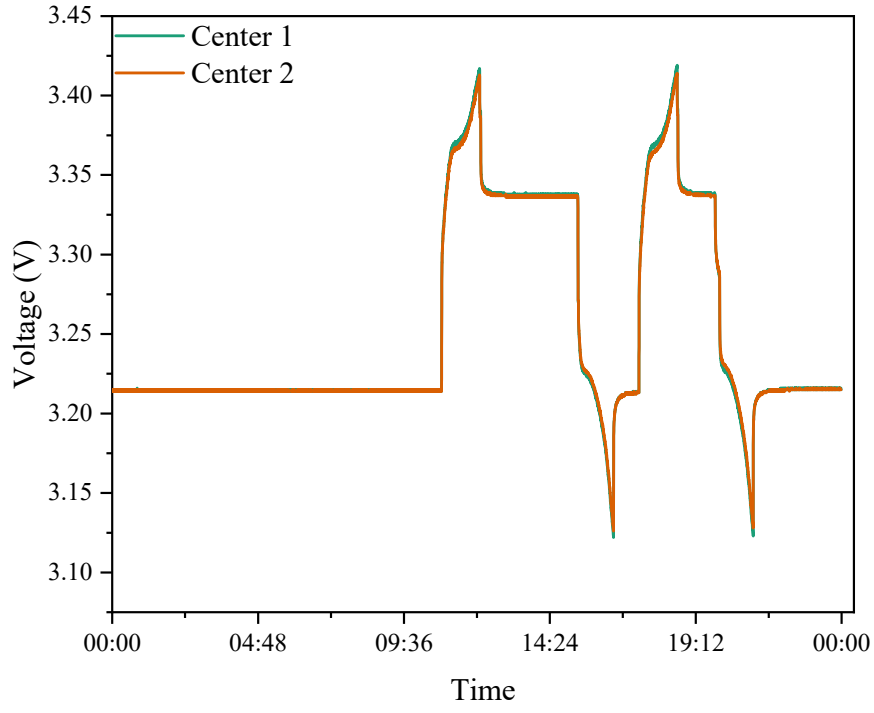


Figure 3. Voltage centroid-like curves for each cell in the cell cluster.

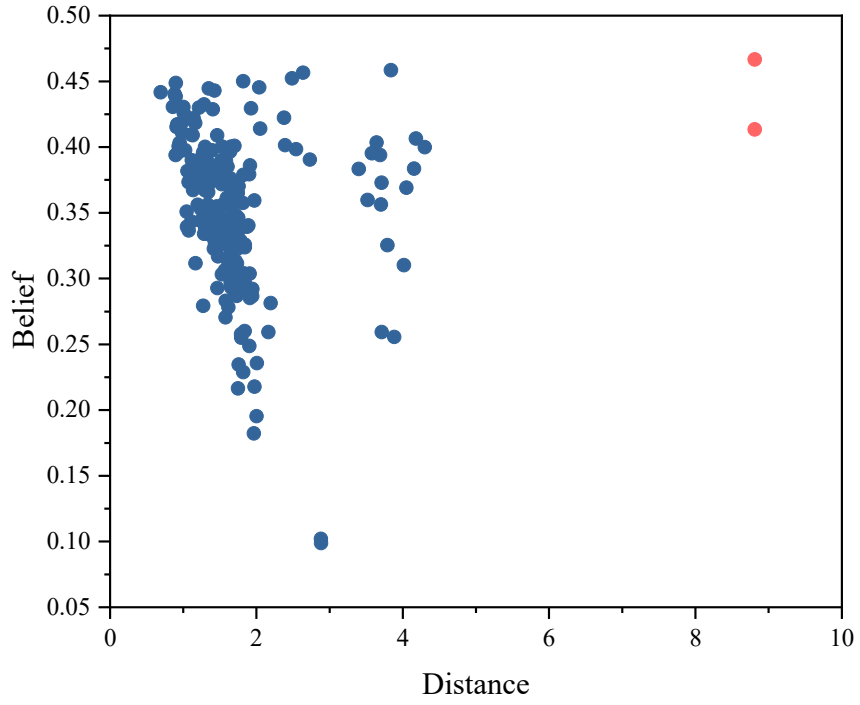


Figure 4. Voltage centroid-like curves for each cell within the cell cluster (2 h).

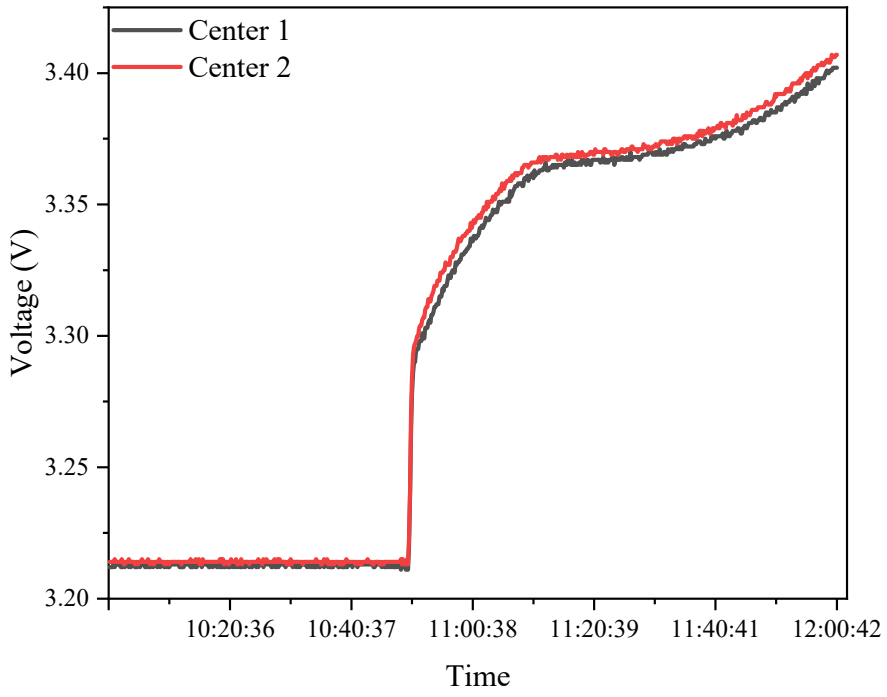


Figure 5. Voltage centroid-like curves for each cell in the battery cluster during charging time (2 h).

5.3. EKNN-Based Cell Parameter Classification

Clustering analysis was performed on 90% of the core parameters, and the remaining 10% were classified using the EKNN algorithm. This process was repeated ten times, and the results of m (Ω) are shown in Figure 6. As illustrated in the figure, all battery cells demonstrate low values of m (Ω), suggesting that these batteries are likely to belong to either Class I or Class II, exhibiting relatively consistent performance.

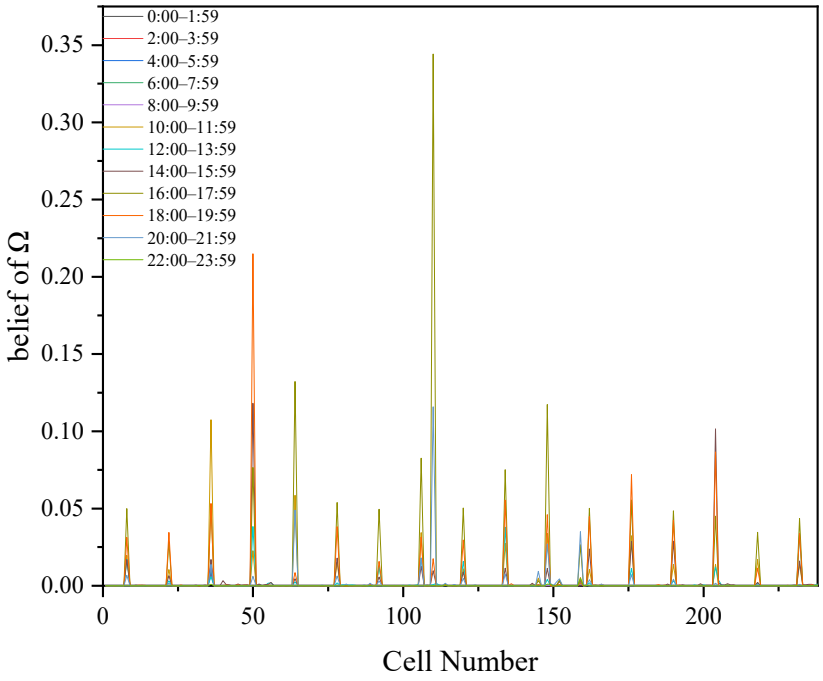


Figure 6. Consistency results of energy storage test cells.

To facilitate a comparative analysis, the same dataset is examined through the framework of the extreme value method, a widely adopted approach in contemporary engineering practices. The method for diagnosing battery consistency involves the comparison of the voltage value of a designated cell to the mean voltage of the other cells. The absolute value of the difference between the two is then calculated. A threshold for voltage difference is defined, and if the voltage difference exceeds this threshold, the alarm is activated. In the event that the measurement remains below the established threshold, the batteries are considered consistent. The 238 cells in the first battery cluster are analyzed using the differential approach, generating the differential values depicted in Figure 7. As demonstrated in the accompanying figure, the maximum differential value attained is 0.0029 V. An analysis of the 238 cells in the first battery cluster using the difference method yielded the differences shown in Figure 7. As demonstrated in the figure, the maximum observed discrepancy is 0.029 V. Once the threshold is set to 0.02 V, 17 cells are identified as inconsistent, with the following serial numbers: 8, 22, 36, 50, 78, 92, 106, 110, 120, 134, 148, 162, 176, 190, 204, 218, 232. Concurrently, an analysis of the cells of all seven battery clusters is conducted using the BPEC-EKNN algorithm and interpolation methods to identify inconsistent battery cells, respectively. The results are presented in Table 1.

Table 1. Comparison of serial numbers of inconsistent battery cells of BPEC-EKNN and differential method.

Battery Cluster	BPEC-EKNN	Differential Method (Threshold = 0.04)	Differential Method (Threshold = 0.05)
1	/	/	/
2	/	/	/
3	108	108	/
4	32	15–17, 19, 21, 22, 28, 32, 43, 45, 47, −52, 47–52, 54, 56	22, 32, 50
5	78, 93	36, 71–84, 93, 161, 232	71–81, 93, 161
6	155, 157, 159, 162, 164, 166, 196	145, 157, 159, 160, 161, 162, 164, 165, 166, 167, 196	145, 196
7	149, 162, 190	8, 22, 95, 149, 162, 185, 188, 190, 191, 194	149, 190

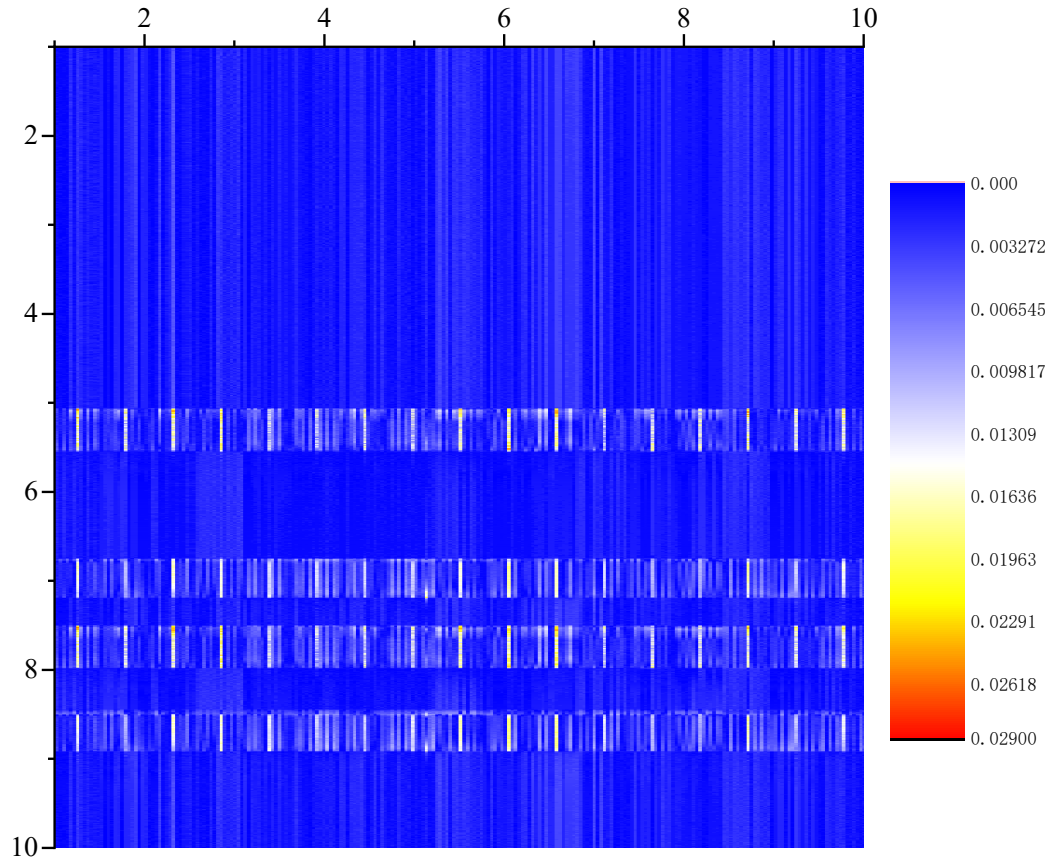


Figure 7. Differential values of cells.

To demonstrate the reliability of the consistency monitoring results obtained by this algorithm, a comparison is conducted between inconsistent and consistent battery cells within the fourth battery cluster. The comparison results are shown in Figure 8. As illustrated, the monitored cell no. 32 indeed exhibits significant inconsistency, with its voltage value showing a substantial abnormal increase upon reaching the charging peak.

As illustrated in Table 1, the differential method necessitates the determination of a threshold value. The magnitude of this value subsequently determines the number of inconsistent battery cells identified. In the event that the threshold is established at an elevated level, fewer battery cells are detected as being inconsistent. Conversely, if the threshold is established at a lower level, a greater number of battery cells are identified as being inconsistent. To illustrate, for the 5th battery cluster, when the threshold is set to 0.04, the series of battery cells from 71 to 84 are detected. The voltage curves of these materials are depicted in Figure 9. As illustrated in the figure, with the exception of cell 78 (the topmost curve), all other cells demonstrate a high degree of consistency and thus do not meet the criteria for being considered inconsistent cells. Furthermore, the results of the consistency monitoring of the 7th battery cluster indicate that the BPEC-EKNN method detected inconsistencies in battery no. 162. Conversely, the difference method failed to identify this curve when the threshold was set to 0.05.

To further validate the effectiveness of the BPEC-EKNN algorithm in consistency diagnostics and analyze the impact of the selected time window span on consistency monitoring results, this paper employs a 24 h time window for consistency monitoring. Following the implementation of parameter adjustments deemed necessary for the purpose of achieving the desired outcome, the results of the consistency monitoring for the 7th battery cluster on a daily basis are presented in Figure 10. The figure indicates that when the time span is altered to a 24 h cycle, only two inconsistent battery elevators are

detected: battery no. 162 and no. 190. These results demonstrate that the selected time span range exerts a significant influence on monitoring outcomes. As the time span increases, the monitoring accuracy concomitantly diminishes.

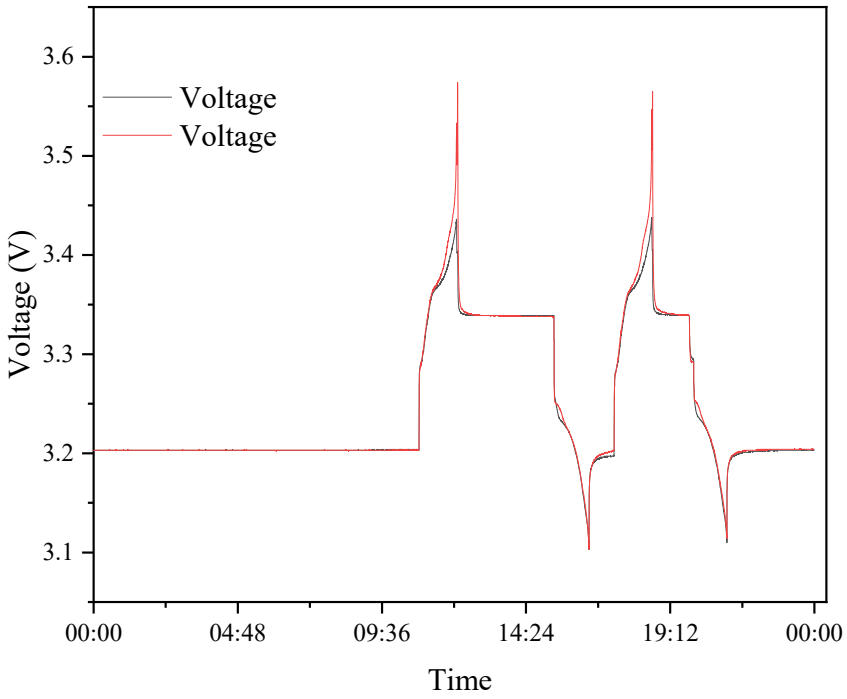


Figure 8. Voltage curves for cell 32 of cluster 4.

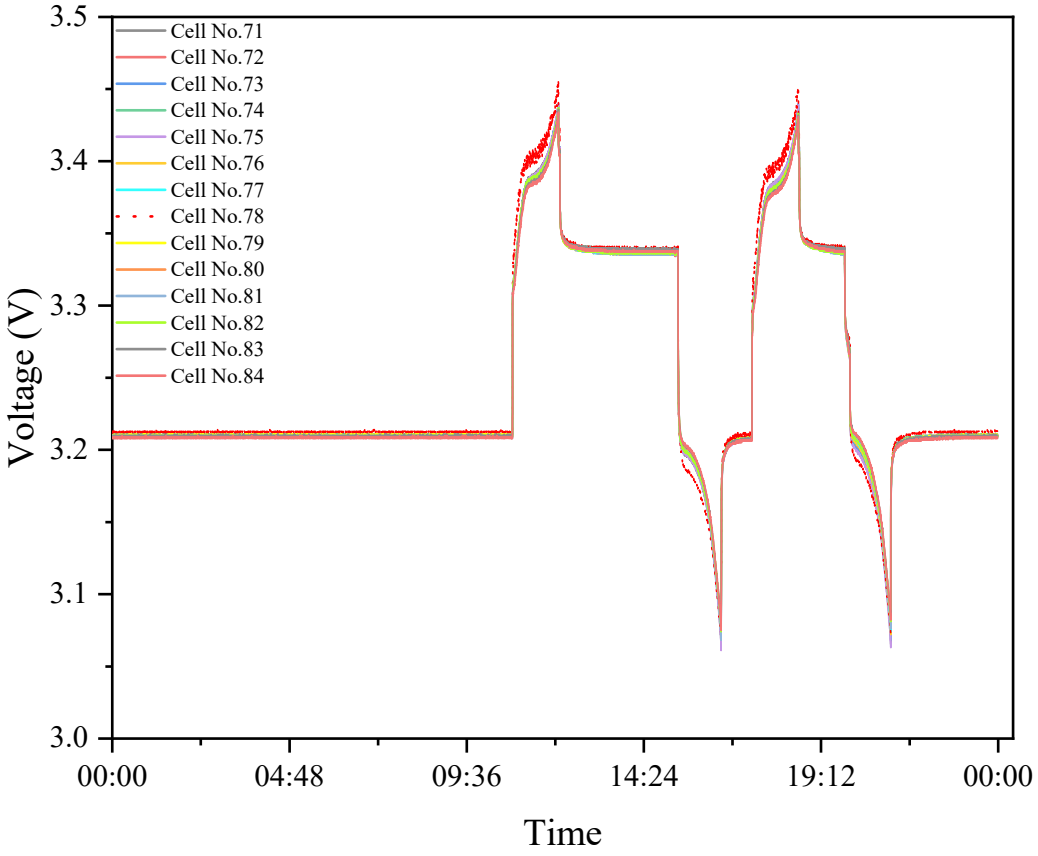


Figure 9. Voltage curves for cells 71–84.

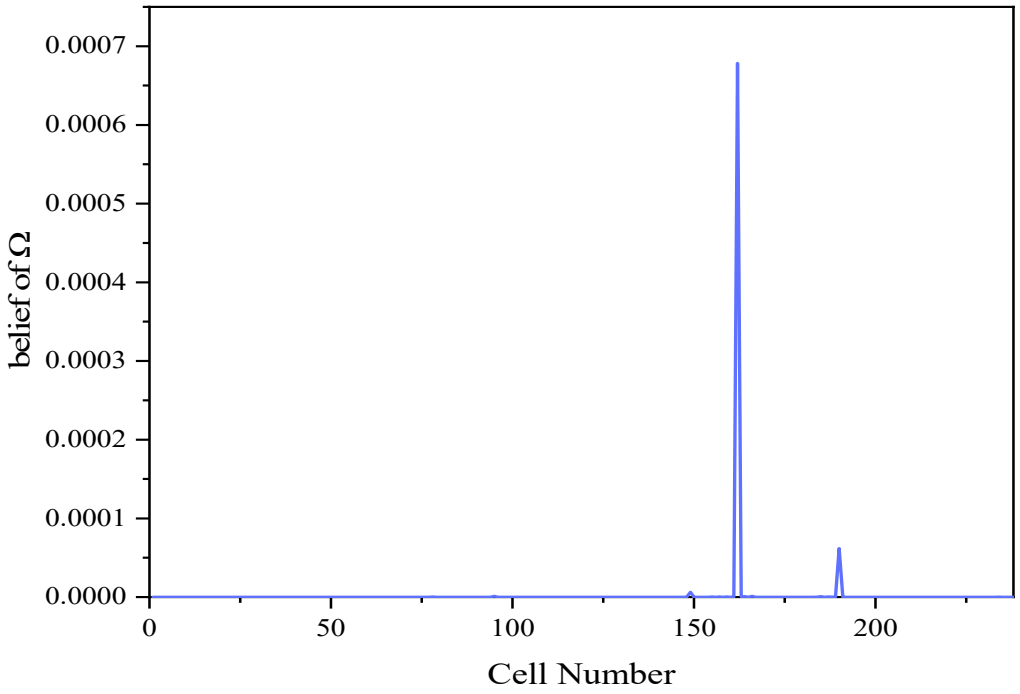


Figure 10. Consistency results of energy storage with a 24 h time span.

6. Conclusions and Recommendations

6.1. Conclusions

This paper takes the energy storage system as the research object and proposes a consistency detection method based on the framework of clustering-classification for the inconsistency of the state of the electric cores in the energy storage system, in which the clustering algorithm adopts Belief Peaks Evidential Clustering (BPEC) and the classification algorithm adopts Evidential K-Nearest Neighbors (EKNN). The BPEC algorithm is used to cluster the core characteristic parameters under the time series data, analyze the category attributes of each core, judge the overall consistency level of the core, and form the core evidence base. Second, based on the core evidence base, the EKNN algorithm is used to categorize the test cores to judge the cores belonging to different categories and the confidence of the overall identification framework. The confidence of belonging to the identification framework is the consistency evaluation index adopted in this paper, which is also called the identification framework evidence. Finally, according to the value of the identification framework evidence, the consistency level of the core is judged, and a large identification framework evidence indicates that the possibility of the core being an inconsistent core is high; otherwise, the possibility of the core being an inconsistent core is low.

In order to verify the effectiveness of the BPEC-EKNN algorithm, this paper adopts the energy storage system in Jiangsu Jinhu as an example. Overall, the time series battery cell consistency detection method based on BPEC-EKNN proposed in this paper has strong reliability and feasibility, and can realize the consistency diagnosis of battery cells. The proposed method is directed toward diagnosing inconsistent battery cells and providing recommendations to operators for battery replacement. When the inconsistency exceeds 1, the battery requires replacement. The algorithm proposed in this paper is a consistency diagnosis method based on actual operating data. In this study, voltage is selected as the feature parameter, on the basis that it can be obtained in real time and each cell has a corresponding measurement point. Nonetheless, it is vital to emphasize that while the case studies presented herein focus on cell voltages during actual operation, this methodology

remains applicable if alternative representative cell parameters are available. As a data-driven approach, this algorithm necessitates the maintenance of optimal data quality. When data quality deteriorates, such as the case of widespread sensor failures or significant data gaps, the accuracy and reliability of the algorithm simultaneously decrease. Moreover, the data-driven nature of the algorithm precludes its analysis of the underlying causes of inconsistencies in energy storage batteries. Consequently, this algorithm is capable of identifying cells that demonstrate inconsistencies while failing to provide a comprehensive analysis of the underlying causes of these inconsistencies and the consequent alterations in voltage curves.

Therefore, experimental verification is required to determine the specific mechanisms and components of the inconsistencies detected. We will conduct further research based on this point in the future.

6.2. Limitations and Practical Enhancement Strategies

Although the proposed BPEC-EKNN method demonstrates high reliability under the current operational dataset, its data-driven nature implies sensitivity to data quality. Scenarios involving widespread sensor failures, substantial missing data segments, or high noise levels may impair clustering performance and evidence fusion, resulting in reduced detection accuracy or inflated ignorance masses m (Ω).

To improve practical applicability, the following enhancement strategies are recommended: (1) robust data preprocessing using temporal-aware imputation or denoising techniques; (2) adaptive tuning of evidence discount rates based on real-time data quality assessment; (3) fusion of multi-parameter evidence (e.g., voltage, temperature, and current) to compensate for single-signal degradation; and (4) implementation of a hybrid fallback mechanism that activates simple threshold-based alarms when data quality drops critically. Future research will focus on validating these strategies on datasets with artificially injected faults and real fault records from operational energy storage stations.

Author Contributions: Conceptualization, Z.L.; methodology, Z.L.; software, Z.L.; validation, Z.L. and N.W.; investigation, Z.L.; data curation, Z.L.; writing—original draft preparation, Z.L. and N.W.; writing—review and editing, Z.L. and N.W.; visualization, Z.L.; supervision, N.W.; project administration, Z.L. and N.W.; funding acquisition, N.W. All authors have read and agreed to the published version of the manuscript.

Funding: This paper is funded by the Science and Technology Research and Development Project of State Grid Integrated Energy Service Group Co., Ltd. (grant number: 527899240001).

Data Availability Statement: The original contributions presented in this study are included in the article. Further inquiries can be directed to the corresponding author.

Conflicts of Interest: Author Zhen Li and Nan Wang were employed by the company State Grid Integrated Energy Services Group Limited. The remaining authors declare that the research was conducted in the absence of any commercial or financial relationships that could be construed as a potential conflict of interest. The authors declare that this study received funding from the Sciences and Technology Research and Development Project of State Grid Integrated Energy Service Group Limited. The funder was not involved in the study design, collection, analysis, interpretation of data, the writing of this article or the decision to submit it for publication.

References

1. Olabi, A.G.; Abdelkareem, M.A. Energy storage systems towards 2050. *Energy* **2021**, *219*, 119634. [CrossRef]
2. Abdi, H.; Mohammadi-ivatloo, B.; Javadi, S.; Khodaei, A.R.; Dehnavi, E. Energy storage systems. In *Distributed Generation Systems*; Elsevier: Amsterdam, The Netherlands, 2017; Chapter 7; pp. 333–368.
3. Amrouche, S.O.; Rekioua, D.; Rekioua, T.; Bacha, S. Overview of energy storage in renewable energy systems. *Int. J. Hydrogen Energy* **2016**, *41*, 20914–20927. [CrossRef]

4. Mitali, J.; Dhinakaran, S.; Mohamad, A.A. Energy storage systems: A review. *Energy Storage Sav.* **2022**, *1*, 166–216. [CrossRef]
5. Yang, Y.; Bremner, S.; Menictas, C.; Kay, M. Battery energy storage system size determination in renewable energy systems: A review. *Renew. Sustain. Energy Rev.* **2018**, *91*, 109–125. [CrossRef]
6. Olabi, A.G. Renewable energy and energy storage systems. *Energy* **2017**, *136*, 1–6. [CrossRef]
7. Yu, X.; Chen, R.; Gan, L.; Li, H.; Chen, L. Battery safety: From lithium-ion to solid-state batteries. *Engineering* **2023**, *21*, 9–14. [CrossRef]
8. Ouyang, D.; Weng, J.; Chen, M.; Wang, J.; Wang, Z. Sensitivities of lithium-ion batteries with different capacities to overcharge/over-discharge. *J. Energy Storage* **2022**, *52*, 104997. [CrossRef]
9. Gotz, J.D.; Teixeira, M.A.S.; Corrêa, F.C.; Viana, E.R.; Badin, A.A.; Borsato, M. The Influence of Overcharging and Over-Discharging on the Capacity Degradation of Lithium-Ion Batteries. In Proceedings of the 2024 IEEE Vehicle Power and Propulsion Conference (VPPC), Washington, DC, USA, 7–10 October 2024; IEEE: New York, NY, USA; pp. 1–6.
10. Sherri, M.; Tadepalli, S.; Otto, S.; Lenneman, A.; Babcock, N. Optimizing fault detection in battery energy storage systems through data-driven modeling. *J. Energy Storage* **2025**, *121*, 116466. [CrossRef]
11. Tian, J.; Fan, Y.; Pan, T.; Zhang, X.; Yin, J.; Zhang, Q. A critical review on inconsistency mechanism, evaluation methods and improvement measures for lithium-ion battery energy storage systems. *Renew. Sustain. Energy Rev.* **2024**, *189*, 113978. [CrossRef]
12. Jin, W.; Li, X.; Hui, D.; Li, J.; Qi, W.; Lü, C. Study on statistical characteristics of battery consistency in large-scale energy storage power stations. *Power Gener. Technol.* **2021**, *42*, 298–305.
13. Tursun, K.; Li, M.; Zheng, Y.; Zong, S. Research on Comprehensive Assessment Method of Battery Consistency Based on Scaled Energy Storage Power Station. In Proceedings of the 2024 9th Asia Conference on Power and Electrical Engineering (ACPEE), Shanghai, China, 11–13 April 2024; IEEE: New York, NY, USA; pp. 92–96.
14. Li, G.; Kong, J.; Song, L.; Zhu, Y.; Liu, M.; Liu, C.; Wang, J. Study on voltage consistency characteristics of lithium-ion battery energy storage system. *J. Phys. Conf. Ser.* **2024**, *2788*, 012050. [CrossRef]
15. Nikolaidis, P.; Poullikkas, A. A comparative review of electrical energy storage systems for better sustainability. *J. Power Technol.* **2017**, *97*, 220–245.
16. Wang, Z.; Song, C.; Zhang, L.; Zhao, Y.; Liu, P.; Dorrell, D.G. A data-driven method for battery charging capacity abnormality diagnosis in electric vehicle applications. *IEEE Trans. Transp. Electrif.* **2021**, *8*, 990–999. [CrossRef]
17. Li, X.; Jiang, J.; Wang, L.Y.; Chen, D.; Zhang, Y.; Zhang, C. A capacity model based on charging process for state of health estimation of lithium ion batteries. *Appl. Energy* **2016**, *177*, 537–543. [CrossRef]
18. Pandžić, H.; Bobanac, V. An accurate charging model of battery energy storage. *IEEE Trans. Power Syst.* **2018**, *34*, 1416–1426. [CrossRef]
19. Hou, J.; Gao, T.; Yang, Y.; Wang, X.; Yang, Y.; Meng, S. Battery inconsistency evaluation based on hierarchical weight fusion and fuzzy comprehensive evaluation method. *J. Energy Storage* **2024**, *84*, 110878. [CrossRef]
20. Wang, S.; Wang, Y.; Soo, Y.Y. Evaluation and prediction of lithium-ion battery pack inconsistency in electric vehicles based on actual operating data. *Energy* **2025**, *319*, 134879. [CrossRef]
21. Jia, C.; Liu, W.; He, H.; Chau, K. Superior energy management for fuel cell vehicles guided by improved DDPG algorithm: Integrating driving intention speed prediction and health-aware control. *Appl. Energy* **2025**, *394*, 126195. [CrossRef]
22. Jia, C.; Liu, W.; He, H.; Chau, K. Deep reinforcement learning-based energy management strategy for fuel cell buses integrating future road information and cabin comfort control. *Energy Convers. Manag.* **2024**, *321*, 119032. [CrossRef]
23. Rodriguez, A.; Laio, A. Clustering by fast search and find of density peaks. *Science* **2014**, *344*, 1492–1496. [CrossRef]
24. Wei, X.; Peng, M.; Huang, H.; Zhou, Y. An overview on density peaks clustering. *Neurocomputing* **2023**, *554*, 126633. [CrossRef]
25. Su, Z.; Denoeux, T. BPEC: Belief-peaks evidential clustering. *IEEE Trans. Fuzzy Syst.* **2018**, *27*, 111–123. [CrossRef]
26. Dempster, A.P. Upper and lower probabilities induced by a multivalued mapping. In *Classic Works of the Dempster-Shafer Theory of Belief Functions*; Springer: Berlin/Heidelberg, Germany, 2008; pp. 57–72.
27. Shafer, G. *A Mathematical Theory of Evidence*; Princeton University Press: Princeton, NJ, USA, 1976.
28. Tong, Z.; Xu, P.; Denoeux, T. An evidential classifier based on Dempster-Shafer theory and deep learning. *Neurocomputing* **2021**, *450*, 275–293. [CrossRef]

Disclaimer/Publisher's Note: The statements, opinions and data contained in all publications are solely those of the individual author(s) and contributor(s) and not of MDPI and/or the editor(s). MDPI and/or the editor(s) disclaim responsibility for any injury to people or property resulting from any ideas, methods, instructions or products referred to in the content.